The AAPS Journal (2023) 25:40
https://doi.org/10.1208/s12248-023-00800-x

RESEARCH ARTICLE

In Vitro-In Vivo Extrapolation and Scaling Factors for Clearance of Human and Preclinical Species with Liver Microsomes and Hepatocytes

David Tess[1] · George C. Chang[2] · Christopher Keefer[2] · Anthony Carlo[3] · Rhys Jones[4] · Li Di[5]

Received: 26 January 2023 / Accepted: 3 March 2023 / Published online: 13 April 2023

Abstract

In vitro-in vivo extrapolation ((IVIVE) and empirical scaling factors (SF) of human intrinsic clearance (CL_{int}) were developed using one of the largest dataset of 455 compounds with data from human liver microsomes (HLM) and human hepatocytes (HHEP). For extended clearance classification system (ECCS) class 2/4 compounds, linear SFs (SF_{lin}) are approximately 1, suggesting enzyme activities in HLM and HHEP are similar to those *in vivo* under physiological conditions. For ECCS class 1A/1B compounds, a unified set of SFs was developed for CL_{int}. These SFs contain both SF_{lin} and an exponential SF (SF_{β}) of fraction unbound in plasma ($f_{u,p}$). The unified SFs for class 1A/1B eliminate the need to identify the transporters involved prior to clearance prediction. The underlying mechanisms of these SFs are not entirely clear at this point, but they serve practical purposes to reduce biases and increase prediction accuracy. Similar SFs have also been developed for preclinical species. For HLM-HHEP disconnect (HLM > HHEP) ECCS class 2/4 compounds that are mainly metabolized by cytochrome P450s/FMO, HLM significantly overpredicted *in vivo* CL_{int}, while HHEP slightly underpredicted and geometric mean of HLM and HHEP slightly overpredicted *in vivo* $CL_{int.}$ This observation is different than in rats, where rat liver microsomal CL_{int} correlates well with *in vivo* CL_{int} for compounds demonstrating permeability-limited metabolism. The good CL_{int} IVIVE developed using HLM and HHEP helps build confidence for prospective predictions of human clearance and supports the continued utilization of these assays to guide structure–activity relationships to improve metabolic stability.

Keywords clearance prediction · fraction unbound in plasma · hepatocytes · liver metabolism · microsomes · IVIVE · scaling factor

Abbreviations

ADME	Absorption, distribution, metabolism, and excretion
AFE	Average fold error
ALQ	Above the limit of quantification
BLQ	Below the limit of quantification
CL_h	Hepatic clearance
CL_{int}	Intrinsic clearance
CO_2	Carbon dioxide
CYP	Cytochrome P450
DDI	Drug-drug interaction
$DI_{90\%}$	Total deviation index (a measure of the fold range that captures 90% of prediction errors)
ECCS	Extended clearance classification system
ELogD	Chromatographic LogD
FMO	Flavin-containing monooxygenase
$f_{u,lm}$	Fraction unbound in liver microsomes
$f_{u,p}$	Fraction unbound in plasma
HEK-293	Immortalized human embryonic kidney cell line
HEP	Hepatocytes
HHEP	Human hepatocytes

✉ Li Di
Li.Di@Pfizer.Com

1 Modeling and Simulation, Pfizer Worldwide Research and Development, Cambridge, MA, USA

2 Modeling and Simulation, Pfizer Worldwide Research and Development, Groton, CT, USA

3 Discovery Sciences, Pfizer Worldwide Research and Development, Groton, CT, USA

4 Pharmacokinetics, Dynamics and Metabolism, Pfizer Worldwide Research and Development, La Jolla, CA, USA

5 Pharmacokinetics, Dynamics and Metabolism, Pfizer Worldwide Research and Development, Groton, CT 06340, USA

HLM	Human liver microsomes
HTD 96	96-Well high throughput equilibrium dialysis device
IV	Intravenous
IVIVE	*In vitro-in vivo* Extrapolation
k_w	Chromatographic capacity factor in aqueous
LC–MS/MS	Liquid chromatography with tandem mass spectrometry
LM	Liver microsomes
$logD_{7.4}$	Log_{10} of distribution coefficient between octanol and pH 7.4 buffer
MDCK	Madin-Darby canine kidney cell line
MDCK-LE	Low efflux MDCK cell line (i.e., RRCK)
$MgCl_2$	Magnesium chloride
NADPH	Reduced nicotinamide adenine dinucleotide phosphate
NHP	Non-human primate
OAT	Organic anion transporter
OATP	Organic anion transporting polypeptides
P_{app}	Apparent permeability
PBPK	Physiologically based pharmacokinetic modeling
PBS	Phosphate-buffered saline
PK	Pharmacokinetics
pK_a	Negative log_{10} of acid dissociation constant
R_{bp}	Blood-to-plasma ratio
rpm	Revolutions per minute
RRCK	Ralph and Russ canine kidney cell line (i.e., MDCK-LE)
SAR	Structure-activity relationships
SF	Scaling factor
SF_β	Exponential scaling factor
SF_{lin}	Linear scaling factor
SFLogD	Shake-flask LogD
UV	Ultraviolet

Introduction

Clearance is one of the most important pharmacokinetic (PK) parameters of drug candidates influencing dose, half-life and dosing regimen (1–5). Over the years, human clearance prediction has continued to evolve from using single species or allometric scaling from preclinical species to *in vitro-in vivo* extrapolation (IVIVE) and physiologically based pharmacokinetic (PBPK) modeling (6–15). Our ability to accurately predict human clearance has strengthened due to improvements in the quality of *in vitro* reagents (e.g., human liver microsomes (HLM) and human hepatocytes (HHEP)) and methodologies for clearance measurements (9, 15–24). Metabolism continues to play a major role in the elimination of small molecule drugs in humans, along with renal and biliary clearance and transporter-mediated pathways (25). Due to the major species differences in drug metabolizing enzymes (26), using animals to scale human metabolic clearance is no longer a common practice in modern drug discovery, although scaling from preclinical species is routinely used to predict human oral absorption, steady-state volume of distribution, and renal clearance (27–36). *In vitro* metabolic stability assays using human reagents (e.g., HLM and HHEP) are most frequently applied to predict human *in vivo* clearance, as well as guiding structure–activity relationships (SAR) to improve metabolic stability. Therefore, development of IVIVE and empirical scaling factors (SFs) using these reagents are important to understand the clearance prediction accuracy in humans, minimize prediction biases, and increase success in the clinic (37). We have recently reported clearance IVIVE and SFs for preclinical species using liver microsomes (LM) and hepatocytes (HEP) (38). In this study, we focus on development of human clearance IVIVE and SFs for each class using the extended clearance classification system (ECCS) (39).

Recently, a large collection of human intravenous (IV) PK data of 1352 compounds has been published (40). Using this IV dataset predominately, we generated *in vitro* data for eight different endpoints including physicochemical properties, metabolic stability and other absorption, distribution, metabolism, and excretion (ADME) properties. Here, we discuss using a subset of 455 compounds for development of clearance SFs and IVIVE with HLM and HHEP. This is the largest study of human clearance IVIVE and SFs using consistent *in vitro* assays developed in house. The clearance IVIVE and SFs from preclinical species (38) are updated as well with the new approaches applied to human. The parallel-tube liver clearance model is utilized to develop IVIVE and SFs, as it outperformed the well-stirred liver model for high clearance compounds, and provided only minor differences for low-to-moderate clearance compounds (38). As such, only the parallel-tube liver model is discussed in this manuscript. The IVIVE and SFs developed will enable us to improve the accuracy and our confidence in human clearance and PK prediction.

Materials and Methods

Material

Cryopreserved HHEPs (Lot SPB consisting of 13 donors with 6 male and 7 female, datasheet available in supplemental material) were custom-pooled and prepared by BioIVT (Westbury, NY). HLMs of 50 donor pools (Lot 103 containing 36 male and 14 female donors, datasheet available in supplemental material) were purchased from Xenotech (Kansas City, KS). Cryopreserved male HEPs and male LMs

of CD-1 mouse, Sprague Dawley and Wistar Han rat, beagle dog and cynomolgus monkey were purchased from by BioIVT (Westbury, NY), Lonza (Walkersville, MD), Xeno-Tech (Lenaxa, KS), and Corning (BD Biosciences, Woburn, MA). Frozen plasma and fresh blood were obtained from BioIVT and Pfizer labs (Groton, CT). All chemicals were obtained from Pfizer Global Material Management (Groton, CT) or purchased from Sigma-Aldrich (St. Louis, MO) unless specified otherwise. The 96-well equilibrium dialysis (HTD 96) device and cellulose membranes with molecular weight cut-off of 12–14 K were obtained from HTDialysis, LLC (Gales Ferry, CT).

In Vitro Data

The detailed protocols have been discussed previously on the microsomal and hepatocyte stability assays, permeability assay and assays for binding (i.e., plasma and liver microsomes), blood-to-plasma ratio, $logD_{7.4}$ and pK_a measurements (17, 38). Briefly, for liver microsomal stability experiments, test compounds (1 µM) were incubated with liver microsomes (LMs, 0.25 µM CYP protein) for 1 h in the presence of NADPH (1.3 mM), $MgCl_2$ (3.3 mM), and potassium phosphate buffer (100 mM at pH 7.4). For hepatocyte stability experiments, test compounds (1 µM) were incubated with hepatocytes at 0.5 million cells/mL at 37°C in an incubator (relative humidity ≥ 90%, 5% CO_2/air) for 4 h. Hepatocytes maintained functional activity during the experimental of 4-h incubation (41). At various time points, samples were taken, proteins were precipitated with cold acetonitrile containing internal standards, and supernatants were analyzed by LC–MS/MS. CL_{int} was calculated based on loss of parent compounds over time using equations discussed in a previous paper (38). A hepatocyte relay assay was used for low clearance compounds at cell densities of 0.5 or 2 million cells/mL (19). Replicate measures of LM and HEP apparent intrinsic clearance ($CL_{int,app}$) were geometrically averaged. Measures below or above the limits of quantification (BLQ and ALQ) were geometrically averaged with quantified values utilizing Beal's method M3 if at least half the replicates were quantifiable (42). For binding measurements in plasma or liver microsomes, test compound (2 µM) was added to the matrices and dialyzed against phosphate buffered saline (PBS) for 6 h using HTD96 equilibrium dialysis device in a CO_2 incubator (75% relative humidity, 200 rpm) at 37°C (38). At the end of the dialysis, samples were matrix-matched and analyzed by LC–MS/MS. Fraction unbound values were calculated using equations presented in the previous publication (38). Apparent permeability (P_{app}) was measured using the low efflux MDCK cells (MDCK-LE, i.e., RRCK) in a 96-transwell® monolayer assay (43). Test compounds (2 µM) in a cassette format ($n = 4$) were added to the donor wells and buffer in the receiver wells. After 1.5-h incubation (95% humidity, 5% CO_2/air) at 37°C, samples were analyzed using LC–MS/MS. P_{app} was calculated using equations described in the previous publication (38, 43). Blood-to-plasma ratio was determined by adding test compound (1 µM) in fresh blood and incubating at 37°C for both 1 and 3 h in an incubator (90% humidity, 5% CO_2/air) on a shaker (450 rpm) (44). At the end of the incubations, plasma was separated from blood. Blood and plasma samples were matrix-matched, quenched with cold acetonitrile containing internal standards and centrifuged, and supernatants were analyzed by LC–MS/MS. PFLogD (45) was calculated using an in-house LogD model that was developed to predict LogD for any compounds based on underlying experimental data from the SFLogD (46) and ELogD (47) assays. PFLogD calculations take into account the known limitations of the SFLogD (inaccurate for compounds with actual LogD above 4.0) and ELogD (inadequate for acidic or zwitterionic compounds) assays by performing a logical combination of the results from the two assays based on the chemical space of the compound being predicted. In a SFLogD experiment, test compound (67 µM) was added to a 96 well-plate containing octanol/phosphate buffer (pH 7.4) in a 1:1 ratio pre-saturated with one another (46, 48). The plate was sealed and mixed on a plate shaker for 15 min at room temperature. At the end of the experiment, the octanol and buffer phases were separated by centrifugation and the samples were analyzed by LC–MS/MS. The $\log_{10}$ of compounds in octanol divided by those in buffer is LogD. The ElogD method measured the chromatographic retention time of test compounds in the presences of a small amount of octanol and various amount of methanol in the mobile phase (47). The chromatographic capacity factor [(compound retention time − retention time of solvent)/retention time of solvent] was extrapolated to 100% aqueous (k_w') and correlations between LogD and k_w' was developed using compounds with known LogD. This relationship between LogD and k_w' was then used to calculate ElogD (47). pKa was measured using a capillary electrophoresis method (49, 50). Electrophoretic separations were performed in parallel across 24 different pH buffers (pH 1.8–11.2) for test compounds to measure migration time relative to a neutral marker (DMSO) using UV detection. Titration curves were generated on effective mobility *vs.* pH to calculate pKa. The MoKa software (Molecular Discovery Limited, London, UK) was used to calculate pKa, when experimental data were not available.

In Vivo IV PK Data

Human IV PK data are mostly from the literature (40) and animal IV PK data were obtained using protocols described previously (38). All procedures performed on these animals were in accordance with regulations and established guidelines and were reviewed and approved by an Institutional Animal

Care and Use Committee or through an ethical review process. For ECCS class 4A compounds predominantly eliminated by renal clearance ($logD_{7.4} \leq 2$), hepatic clearance data were not included in the analysis for this class if renal clearance values were not available. Renal clearance was assumed to be negligible for the remaining ECCS classes (i.e., 1A, 1B, 2, and 4B) if not available. The assumption is reasonable, as these compounds have high passive permeability or LogD and renal reabsorption is likely to be high. Class 3A/3B compounds were excluded from analysis as biliary clearance can be the major clearance mechanism for this class that neither HLM nor HHEP can predict. The parallel-tube model was used to convert between hepatic blood clearance ($CL_{h(b)}$) and CL_{int} (Eq. 1).

$$CL_{h(b)} = Q_h \bullet \left(1 - \exp\left(\frac{-f_{u,p} \bullet CL_{int}}{(R_{bp} \bullet Q_h)}\right)\right) \tag{1}$$

Data Analysis

Average fold error (AFE; aka Bias) was used to assess model prediction accuracy, i.e., the extent of any systematic prediction bias. AFE and its corresponding 90% confidence interval ($AFE_{CI90\%}$) and log-transformed standard deviation (σ_{lnAFE}) were calculated with Eqs. 2–4, where Obs_i are the known observations for each compound, $Pred_i$ are the model predictions for each compound, N is the number of compounds; n_i is the number of predictions per compound, and $\Phi^{-1}_{(0.95)}$ is the normal inverse cumulative distribution for 95% probability.

$$AFE = e^{\left\langle \frac{\Sigma\left\{\ln\left(\frac{Obs_i}{Pred_i}\right)\bullet\frac{1}{n_i}\right\}}{N}\right\rangle} \tag{2}$$

$$AFE_{CI_{90\%}} = e^{\left\langle \ln(AFE)\pm\Phi^{-1}_{(0.95)}\frac{\sigma_{lnAFE}}{\sqrt{N}}\right\rangle} \tag{3}$$

$$\sigma_{lnAFE} = \sqrt{\frac{\Sigma\left\{\left(\ln\left(\frac{Obs_i}{Pred_i}\right) - \ln(AFE)\right)^2 \bullet \frac{1}{n_i}\right\}}{N}} \tag{4}$$

The Pearson correlation coefficient (ρ; aka R) of the log transformed observations and predictions was used to assess model prediction precision. ρ and its corresponding 90% confidence interval ($\rho_{CI90\%}$) and Z-transformed standard deviation ($\sigma_{Z\rho}$) were calculated with Eqs. 5–7.

$$\rho = \frac{\Sigma\left\{\left(\ln Obs_i - \frac{\Sigma\left\{\ln Obs_i \frac{1}{n_i}\right\}}{N}\right)\bullet\left(\ln Pred_i - \frac{\Sigma\left\{\ln Pred_i \frac{1}{n_i}\right\}}{N}\right)\frac{1}{n_i}\right\}}{\sqrt{\Sigma\left\{\left(\ln Obs_i - \frac{\Sigma\left\{\ln Obs_i \frac{1}{n_i}\right\}}{N}\right)^2 \frac{1}{n_i}\right\}\bullet\Sigma\left\{\left(\ln Pred_i - \frac{\Sigma\left\{\ln Pred_i \frac{1}{n_i}\right\}}{N}\right)^2 \frac{1}{n_i}\right\}}} \tag{5}$$

$$\rho_{CI_{90\%}} = \frac{e^{\left\langle 2\bullet\left(\frac{\ln\left(\frac{(1+\rho)}{(1-\rho)}\right)}{2} \pm \Phi^{-1}_{(0.95)}\bullet\sigma_{Z\rho}\right)\right\rangle} - 1}{e^{\left\langle 2\bullet\left(\frac{\ln\left(\frac{(1+\rho)}{(1-\rho)}\right)}{2} \pm \Phi^{-1}_{(0.95)}\bullet\sigma_{Z\rho}\right)\right\rangle} + 1} \tag{6}$$

$$\sigma_{Z\rho} = \sqrt{\frac{1}{(N-3)}} \tag{7}$$

Three methods were used to assess model prediction precision and accuracy, absolute average fold error (AAFE), root mean square fold error (RMSFE; aka ε), and percent of predictions within 2-fold the observations (% within 2-fold). AAFE provides the average absolute spread of model prediction error from unity. AAFE and its corresponding 90% confidence interval ($AAFE_{CI90\%}$) and log-transformed standard deviation (σ_{lnAAFE}) are calculated (51) with Eqs. 8–10.

$$AAFE = e^{\left\langle \frac{\Sigma\left\{\left|\ln\left(\frac{Obs_i}{Pred_i}\right)\right|\bullet\frac{1}{n_i}\right\}}{N}\right\rangle} \tag{8}$$

$$AAFE_{CI_{90\%}} = e^{\left\langle \ln(AAFE)\pm\Phi^{-1}_{(0.95)}\frac{\sigma_{lnAAFE}}{\sqrt{N}}\right\rangle} \tag{9}$$

$$\sigma_{lnAAFE} = \sqrt{\frac{\Sigma\left\{\left(\left|\ln\left(\frac{Obs_i}{Pred_i}\right)\right| - \ln(AAFE)\right)^2 \bullet \frac{1}{n_i}\right\}}{N}} \tag{10}$$

RMSFE provides the variance of the model prediction errors from unity. RMSFE and its corresponding 90%

confidence interval ($RMSFE_{CI90\%}$) and log-transformed standard deviation ($\sigma_{\ln\varepsilon}{}^2$) were calculated (51) with Eqs. 11–13.

$$RMSFE = \varepsilon = \sqrt{\frac{\Sigma\left\{\left(\ln\left(\frac{Obs_i}{Pred_i}\right)\right)^2 \bullet \frac{1}{n_i}\right\}}{N}} \tag{11}$$

$$RMSFE_{CI_{90\%}} = \sqrt{e^{\langle \ln(\varepsilon^2) \pm \Phi^{-1}_{(0.95)}\sigma_{\ln\varepsilon^2}\rangle}} \tag{12}$$

$$\sigma_{\ln\varepsilon^2} = \sqrt{\frac{2 \bullet \left(1 - \left(\frac{\Sigma\left\{\ln\left(\frac{Obs_i}{Pred_i}\right) \bullet \frac{1}{n_i}\right\}}{\varepsilon \bullet N}\right)^4\right)}{N-2}} \tag{13}$$

To provide more intuitive meaning to RMSFE values, they were transformed into the total deviation index ($DI_{90\%}$) and the probability within a 2-fold error ($P_{\leq 2\text{-fold}}$). $DI_{90\%}$ is a measure of the fold range that captures 90% of prediction errors. It is basically the 90% confidence interval of the model predictions. $DI_{90\%}$ and its corresponding 90% confidence interval ($DI_{90\%,CI90\%}$) are calculated (51) with Eqs. 14 and 15.

$$DI_{90\%} = e^{\langle \Phi^{-1}_{(0.95)} \bullet \varepsilon \rangle} \tag{14}$$

$$DI_{90\%,CI_{90\%}} = e^{\langle \Phi^{-1}_{(0.95)} \bullet \sqrt{e^{\langle \ln(\varepsilon^2) \pm \Phi^{-1}_{(0.95)} \bullet \sigma_{\ln\varepsilon^2}\rangle}}\rangle} \tag{15}$$

RMSFE can alternatively be transformed into the more intuitive probability of predictions being within 2-fold of observed ($P_{2\text{-fold}}$). $P_{2\text{-fold}}$ and its corresponding 90% confidence interval ($P_{2\text{-fold,CI90\%}}$) are calculated (51) with Eqs. 16 and 17.

$$P_{2\text{fold}} = 1 - \left(1 - \Phi^{-1}_{\left(\frac{\ln 2}{\varepsilon}\right)}\right) \bullet 2 \tag{16}$$

$$P_{2fold,CI_{90\%}} = 1 - \left(1 - \Phi^{-1}_{\left(\frac{\ln 2}{\sqrt{e^{\langle \ln(\varepsilon^2) \pm \Phi^{-1}_{(0.95)} \bullet \sigma_{\ln\varepsilon^2}\rangle}}}\right)}\right) \bullet 2 \tag{17}$$

% within 2-fold was calculated with Eq. 18.

$$\%\text{ within 2-fold} = \frac{\Sigma\begin{cases} 1, e^{\left\langle\left|\ln\left(\frac{Obs_i}{Pred_i}\right)\right|\right\rangle} \leq 2 \\ 0, e^{\left\langle\left|\ln\left(\frac{Obs_i}{Pred_i}\right)\right|\right\rangle} > 2 \end{cases}}{N} \bullet 100\% \tag{18}$$

LM and HEP empirical linear scaling factors (SF_{lin}) were fit in Microsoft Excel by minimizing the -2 log likelihood function (-2LL) per species and ECCS class with lognormal residual error (RMSFE) which negates bias. An additional exponential scaling factor (SF_β) on plasma fraction unbound ($f_{u,p}$) as introduced in Jones *et al.* (20) was additionally considered (Eq. 19). Unlike Jones *et al.* (20), SF_{lin} was limited to positive values (> 0) rather limited to > 1.

$$in\ vivo\ CL_{int} = SF_{lin} \bullet f_{u,p}^{(-SF_\beta)} \bullet in\ vitro\ CL_{int} \tag{19}$$

Scaling factor 95% confidence intervals were determined by log-likelihood profiling. Three significant numbers were used for SFs in order to minimize the likelihood of introducing compounding errors during intermediate calculations using the rounding numbers.

Results

Human hepatic clearance IVIVE and empirical SFs were developed using 448 literature IV clearance values (40) and seven Pfizer drug discovery compounds, after subtracting out renal clearance. *In vitro* physicochemical and ADME data were obtained from Pfizer's internal database. All the *in vitro* and *in vivo* data are included in the Supplemental Material (Excel file, excluding the 7 Pfizer internal compounds). Density plots of the compounds based on their physicochemical and ADME properties are illustrated in Fig. 1. The compounds encompass a wide range of properties and represent typical small molecule drug space. The *in vivo* and *in vitro* data of preclinical species have been published previously (38) with updated analysis using similar approaches as in humans. Only compounds with *in vitro* quantifiable experimental clearance values from LMs and/or HEPs and *in vivo* clearance values were included in the IVIVE analysis. For the other *in vitro* ADME properties (P_{app}, pK_a, $logD_{7.4}$, R_{bp}, $f_{u,p}$, and $f_{u,lm}$), if experimental data were not available, in silico values from internal global QSAR models were judiciously utilized for the analysis on the 455 human compounds. The number of compounds [in brackets] utilizing in silico predictions per *in vitro* assay are: $logD_{7.4}$ [145], pK_a [86], RRCK P_{app} [3], $f_{u,hlm}$ [1], and R_{bp} (1). No in silico predicted $f_{u,p}$ values were used. The in silico predictions are noted in the supplemental excel file with a superscript "1". Compound ECCS class was assigned based on pKa (ionization state), RRCK P_{app}, $LogD_{7.4}$, and MW (Supplemental Material, Word file, Fig. S1) (29, 39). ECCS class 1A compounds are acids or zwitterions with $P_{app} \geq 5 \times 10^{-6}$ cm/s and MW ≤ 400, and class 1B compounds differ from class 1A only by MW > 400. Similarly, class 3A and 3B are acids or zwitterions with low passive permeability ($P_{app} < 5 \times 10^{-6}$ cm/s). Class 2 compounds are bases or neutrals with high passive permeability ($P_{app} \geq 5 \times 10^{-6}$ cm/s).

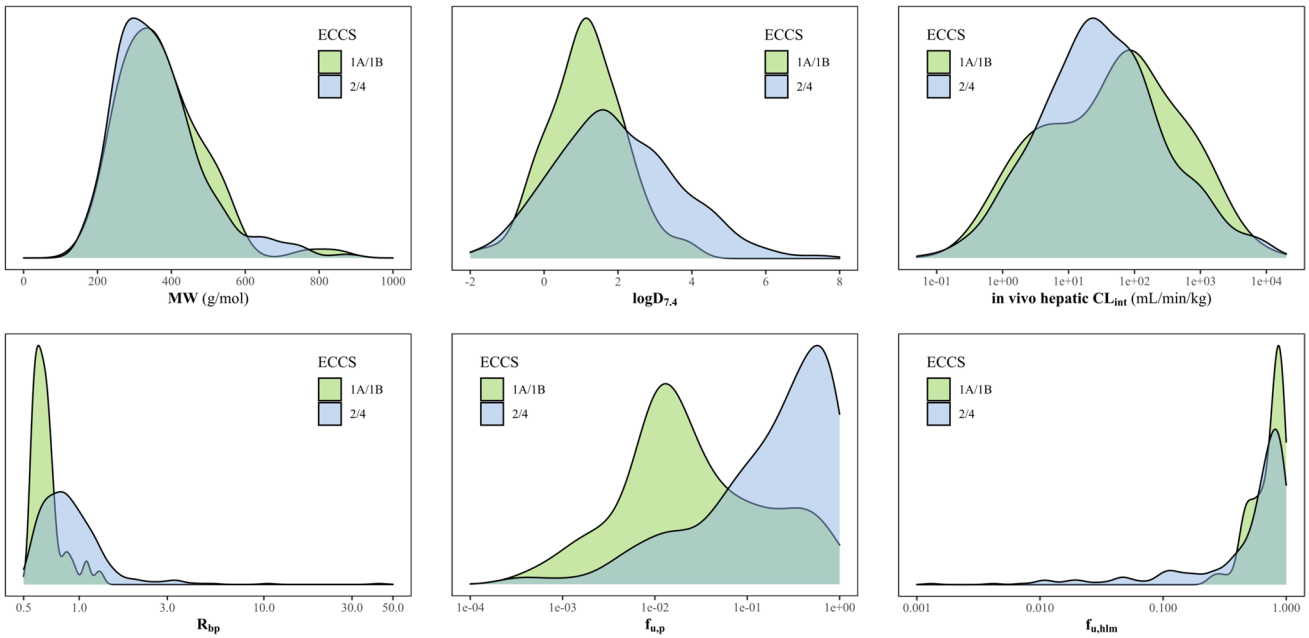

Fig. 1 Density plot of the human IV dataset of 455 compounds based on physicochemical and ADME properties

Class 4A compounds are bases or neutrals with low passive permeability ($P_{app} < 5 \times 10^{-6}$ cm/s) and low lipophilicity ($logD_{7.4} \leq 2$), and class 4B compounds differ from class 4A only by log $D_{7.4} > 2$. Empirical SFs for clearance were developed based on CL_{int} in each ECCS class (39), when there are sufficient compounds in the class ($N > 10$). The physiological parameters used for IVIVE development are summarized in Table I based on previously published information (12) and in house data. It is worth noting that, in the previous analysis of IVIVE and SFs of preclinical species, SIMCYP™ physiological parameters (Certara, Sheffield, UK) values were used instead (38), although they are not meaningfully different than the current values used. For HLM SFs, only compounds predominately metabolized by CYPs and/or FMOs were included.

Human ECCS Class 2/4

ECCS class 2/4 are basic and neutral compounds with metabolic and/or renal clearance as major clearance mechanisms. Most of the Pfizer portfolio compounds belong to these classes. The intrinsic clearance SFs of ECCS class 2/4 were developed with a small set of well-curated compounds (high experimental replicates) that are known to be mainly metabolized by CYPs. With this well-curated dataset, the SF_{lin} is 1.39 ($N=21$, Fig. 2a, Table II) for HLM and 1.12 for HHEP ($N=35$, Fig. 2b, Table II). The confidence intervals for the SFs are summarized in Table II. The SFs are close to 1 for both HLM and HHEP, indicating no significant clearance SFs are needed for this class of compounds. The $DI_{90\%}$ values for both reagents are around 5-fold and other statistical metrices are shown in Table II. Adding an exponential $f_{u,p}$ scalar SF_{β} did not significantly improve the prediction accuracy for this class (data not shown). Applying the linear SFs developed with the well-curated dataset to a large dataset of ECCS class 2/4 compounds results in good IVIVE with minimal over prediction biases for both HLM ($N=91$, bias 1.9-fold, Fig. 2c, CYP/FMO mediated substrates) and HHEP ($N=335$, bias 1.2-fold, Fig. 2d, irrespective of metabolic enzymes). The $DI_{90\%}$ values increased to 8- to 9-fold, which could potentially be due to the noise of the screening data and/or uncertainties in ECCS classification. Other statistical metrices are summarized in Table II.

Table I Physiological Parameters and Experimental Conditions for IVIVE and SF Development

Parameters	Mouse	Rat	Dog	NHP	Human
Q_h (mL/min/kg)	90	70	40	44	20
PRpLW (mg/g)	45	45	45	45	45
HEPpLW (MC/g)	120	135	240	120	120
LWpBW (g/kg)	90	40	32	32	21
PR_{lm} (mg/mL) [a]	0.21	0.34	0.32	0.21	0.8
CD_{hep} (MC/mL) [a]	0.5	0.5	0.5	0.5	0.5 or 2

[a] *In vitro assay conditions*

Q_h, hepatic blood flow; PRpLW, microsomal protein per liver weight; HEPpLW, hepatic cellularity per liver weight; LWpBW, liver weight per body weight; PR_{lm}, liver microsomal protein concentration in incubation; CD_{hep}, hepatocyte cellularity per volume

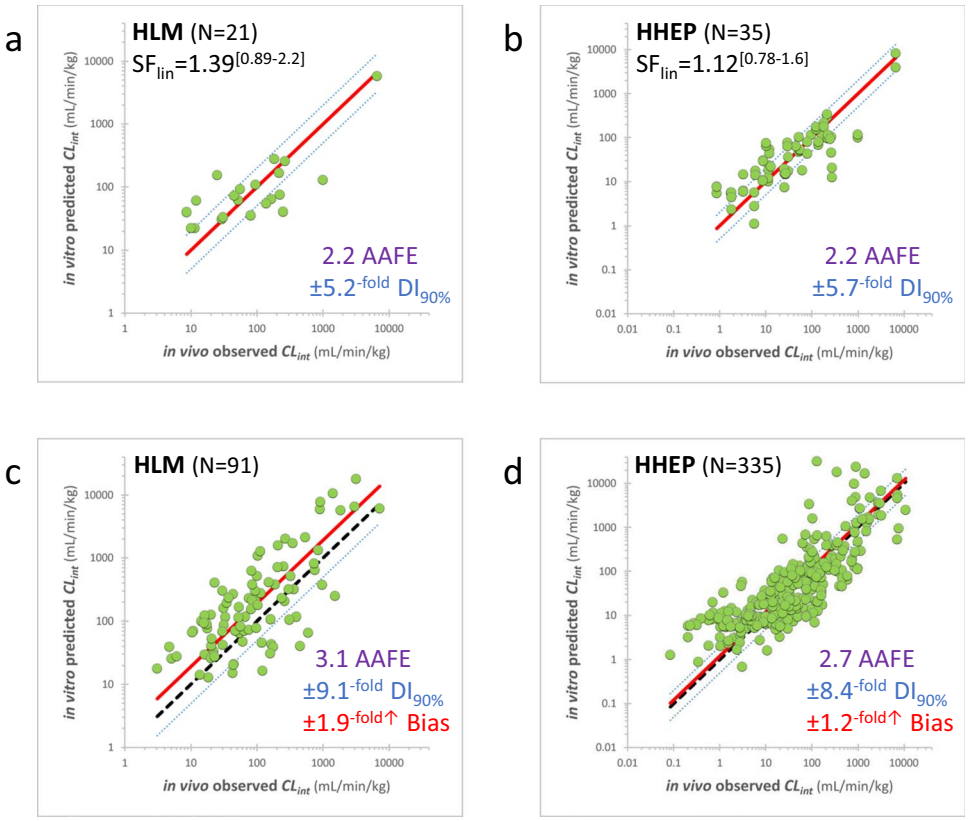

Fig. 2 Human intrinsic clearance IVIVE and scaling factors for ECCS 2/4 compounds. **a** HLM of the well-curated dataset, **b** HHEP of the well-curated dataset, **c** Remaining CYP/FMO substrates of the large dataset in HLM, and **d** Remaining of the large dataset in HHEP

Human ECCS Class 1A/1B

ECCS class 1A/1B compounds are acids and zwitterions with high passive permeability. Uptake transporters are typically involved in clearance of class 1A/1B (Supplemental Material, Fig. S1). When only SF_{lin} is used for class 1A/1B, overprediction of clearance is observed for low clearance compounds, while underprediction is apparent for high clearance compounds (data not shown). Additionally, OATP and OAT2 substrates required different SF_{lin}. The clearance prediction error positively correlated with $f_{u,p}$ (data not shown). Based on this observation and a recent publication on using the SF_{β} for $f_{u,p}$ due to potentially albumin-mediated uptake (20), the SF_{β} was applied to class 1A/1B. With the addition of SF_{β}, prediction accuracy improves significantly, and the prediction error is no longer correlated to $f_{u,p}$. No meaningful overprediction or underprediction are observed for low or high clearance compounds after incorporation of SF_{β}. For class 1A/1B, SF_{lin} and SF_{β} are 0.428 and 0.445, respectively (Fig. 3a, N = 85). The $DI_{90\%}$ is around 6-fold. Additional statistical metrices are summarized in Table II. The reason to develop unified SFs for class 1A and 1B is based on the two classes having very similar SF_{lin} and SF_{β} (data not shown). When the unified SFs are applied to individual classes, they both perform well with minimal biases of 1.3-fold overprediction for class 1A (Fig. 3b) and 1.4-fold underprediction for class 1B (Fig. 3c). Since the likelihood of transporters being involved in class 1A/1B compounds, only HHEP SFs have been developed, as there are no functional transporters in HLM. With the incorporation of SF_{β}, the higher the plasma protein binding (lower $f_{u,p}$), the larger the contribution of $f_{u,p}$ to the overall clearance.

Preclinical Species Clearance IVIVE and Scaling Factors

Clearance IVIVE and linear SF for preclinical species has been developed previously using SIMCYP™ physiological parameters (38). Here, the SFs are updated by including the SF_{β} for class 1A/1B similarly to the approaches for human and incorporating slightly different physiologically parameters historically used in house (12). These results are shown in Fig. 4 for mouse, rat, dog and NHP. Additional statistical metrices are summarized in Supplemental Material Table S1–S4. Both SF_{lin} and SF_{β} for preclinical species and human are summarized in Fig. 5 for each ECCS class.

Prediction of Human Clearance for HLM-HHEP Disconnect Compounds

For certain CYP-mediated compounds, CL_{int} in LM may be greater than observed in HEP (17). The cause for this

Table II Summary of Statistical Metrics of Intrinsic Clearance IVIVE using HLM and HHEP based on ECCS Class

Species	Reagent	ECCS	Compounds	*N*	SF_{lin} [a]	SF_{β} [a]	Bias[b,c] (AFE)	AAFE[b]	$DI_{90\%}$ [b]	$P_{\leq 2\text{-fold}}$ [b]	Within 2-fold	ρ^2 [b] (R^2)
Human	LM	2/4	Training subset	21	$1.39^{[0.89–2.2]}$	$0^{[fixed]}$	$1.0^{\uparrow[0.70–1.4]}$	$2.2^{[1.7–2.7]}$	$5.2^{[3.5–8.7]}$	$51\%^{[40–63\%]}$	52%	$0.60^{[0.32–0.79]}$
		2/4	Remaining CYP/FMO substrates	91	$1.39^{[fixed]}$	$0^{[fixed]}$	$1.9^{\uparrow[1.6–2.3]}$	$3.1^{[2.7–3.5]}$	$9.1^{[7.1–12]}$	$39\%^{[35–44\%]}$	31%	$0.54^{[0.42–65]}$
	HEP	2/4	Training subset	35	$1.12^{[0.78–1.6]}$	$0^{[fixed]}$	$1.0^{\uparrow[0.75–1.3]}$	$2.2^{[1.9–2.7]}$	$5.7^{[4.1–8.4]}$	$49\%^{[41–58\%]}$	55%	$0.68^{[0.50–0.81]}$
		2/4	Remaining	335	$1.12^{[fixed]}$	$0^{[fixed]}$	$1.2^{\uparrow[1.1–1.4]}$	$2.7^{[2.5–2.9]}$	$8.4^{[7.3–9.6]}$	$41\%^{[39–43\%]}$	45%	$0.66^{[0.61–0.71]}$
		1A/1B	All	85	$0.428^{[0.24–0.75]}$	$0.445^{[0.31–0.59]}$	$1.0^{\uparrow[0.83–1.2]}$	$2.5^{[2.2–2.8]}$	$6.3^{[5.1–8.1]}$	$46\%^{[41–52\%]}$	49%	$0.77^{[0.68–0.83]}$
		1A	All	51	$0.428^{[fixed]}$	$0.445^{[fixed]}$	$1.3^{\uparrow[1.0–1.7]}$	$2.5^{[2.1–2.9]}$	$6.6^{[4.9–9.3]}$	$45\%^{[39–52\%]}$	48%	$0.77^{[0.66–0.85]}$
		1B	All	34	$0.428^{[fixed]}$	$0.445^{[fixed]}$	$1.4^{\downarrow[1.0–1.9]}$	$2.4^{[2.0–2.9]}$	$5.9^{[4.2–8.8]}$	$48\%^{[40–57\%]}$	49%	$0.67^{[0.49–0.80]}$

[a] *Scaling factor best fits[95% confidence intervals]*

[b] *Summary statistics[90% confidence intervals]*

[c] *Overprediction bias*$^{\uparrow}$, *underprediction bias*$^{\downarrow}$

disconnect is believed to be mainly due to permeability-limited metabolism in HEP (17), although other factors that have not yet been identified may also contribute to the disconnect. For CYP mediated mechanisms, when intrinsic clearance in HLM is greater than HHEP (≥2-fold to account for assay variability), a decision will need to be made on the assay to use to predict human *in vivo* clearance. For rat, we have previously shown using a dataset of 56 ECCS class 2/4 compounds that LM predicted *in vivo* rat hepatic clearance better than using rat HEP which underpredicted *in vivo* clearance (38). However, in human, this appears different, and there is an observed species difference between rat and human for the disconnect compounds. In human, for the compounds evaluated with HLM CL_{int} greater than HHEP that are predominately metabolized by CYP and/or FMO, HLM overpredicts human *in vivo* hepatic clearance by 2.8-fold ($N=40$, $DI_{90\%}$ 9.7, Fig. 6a, Table III) and HHEP slightly underpredicts *in vivo* clearance by 1.3-fold ($N=40$, $DI_{90\%}$ 4.9, Fig. 6b, Table III). This indicates human *in vivo* hepatocyte permeability is higher than *in vitro*, but still poses some limitations to metabolism (differing in comparison to rat HEP where there appears to be no permeability limitation for *in vivo* metabolism). The geometric mean (geomean) of HLM and HHEP CL_{int} slightly overpredicts *in vivo* human clearance with bias of 1.5-fold and $DI_{90\%}$ of 5.1-fold ($N=40$, Fig. 6c, Table III).

Discussion

This study evaluates human IVIVE and SFs with one of the largest dataset of 455 compounds, consisting of data from standardized *in vitro* assays. The results provide useful insights on prediction accuracy of human clearance. SFs were developed based on ECCS, as different clearance mechanisms required different SFs. Although ECCS was established based on human major clearance mechanisms, similar clearance pathways are likely to occur in preclinical species to some extent (e.g., metabolism *vs.* active transport) (52). As such, the SFs developed for preclinical species were also based on ECCS. SFs for class 3A and 3B were not developed as biliary clearance can be a significant clearance mechanism that neither LMs nor HEPs can predict. SFs are dependent on the compounds involved in their development. There are uncertainties around the SFs, which will need to be considered when defining prediction uncertainty of clearance. For ECCS class 2/4 compounds, the SFs obtained from the well-curated dataset with known clearance mechanisms translate well to the larger dataset (the detailed clearance mechanisms were not investigated) with minimal biases. This provides confidence of using the current reagents for clearance prediction of drug candidates, where clearance

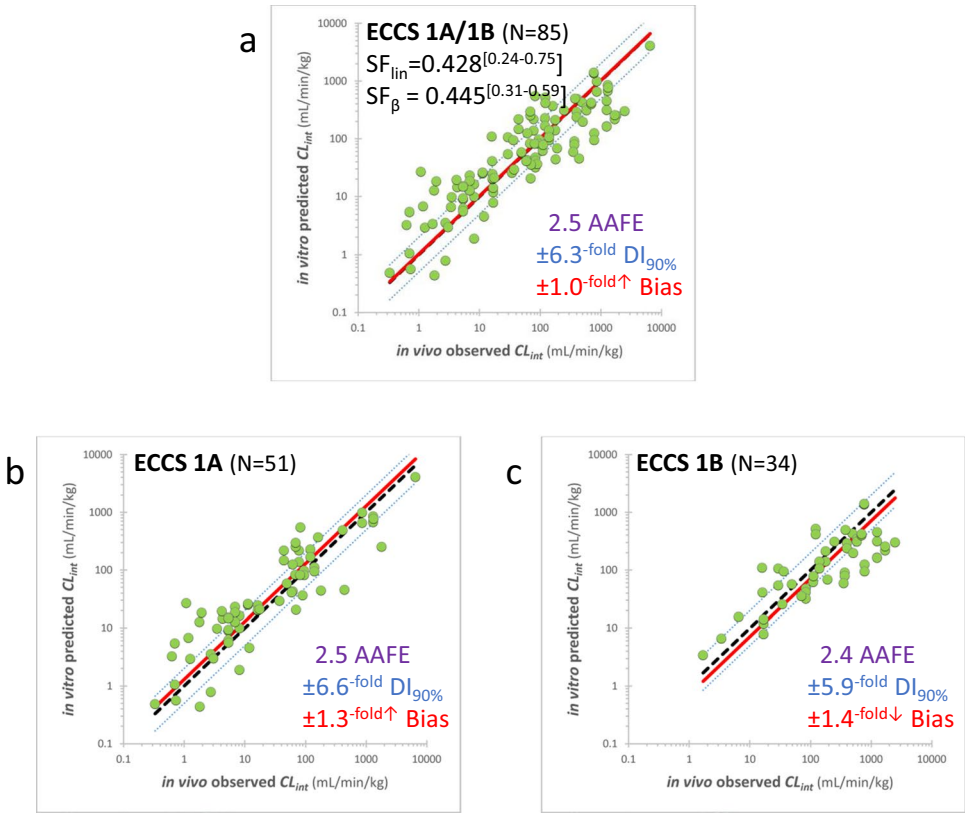

pathways may not have been fully characterized in early drug discovery. When new batches of reagents (LM or HEP) are purchased, IVIVE and SFs will require re-evaluation. The SFs of ECCS class 2/4 compounds are close to 1 using both HLM and HHEP, suggesting the enzyme activities of *in vitro* reagents (i.e., HLM and HHEP) closely represent those in humans under physiological conditions. This is likely credited to judicious selection

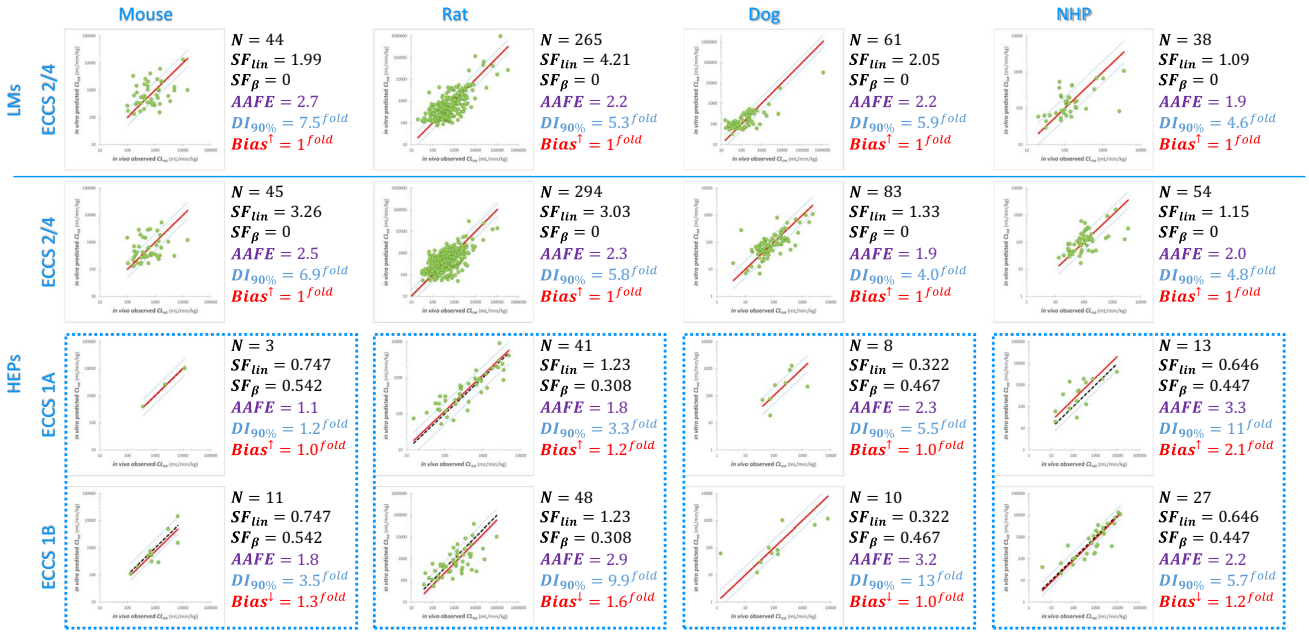

Fig. 4 Intrinsic clearance IVIVE and scaling factors for all ECCS classes of all preclinical species

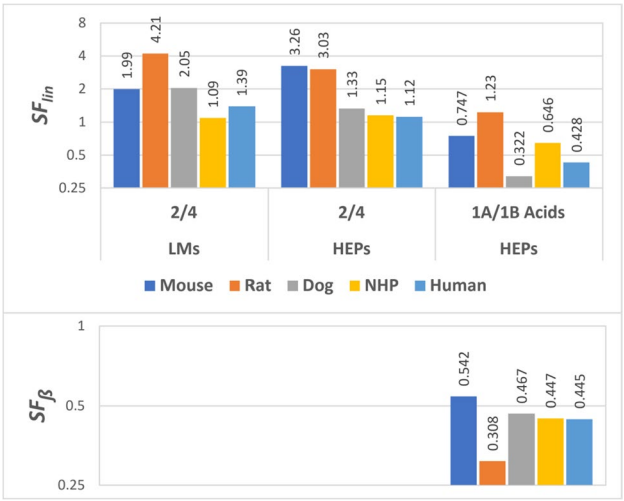

Fig. 5 Summary of intrinsic clearance scaling factors for all ECCS classes of all species

of donors with high enzyme activity similar to human *in vivo* to create the *in vitro* batches, as well as optimal *in vitro* assay conditions. This observation of SFs near unity is in contrary to the literature reports of needing much larger SFs (e.g., 5-fold) for HLM and HHEP to scale human *in vivo* clearance (11, 53), which might potentially be due to lower quality *in vitro* reagents and suboptimal assay conditions from various labs or not considering the impact of ECCS classification for the different clearance mechanisms. Other potential reasons for the higher CL_{int} scaling factor may be due to the use of the well-stirred liver model rather than the parallel-tube model. Reanalysis of the data ($N = 140$, mostly bases and neutrals of ECCS class 2/4 compounds) in the recent publication (54) using parallel-tube model reduced the SFs (Supplemental Material, Table S5). The HLM SF_{lin} (1.49)) in the publication (54) is similar to the SF_{lin} in this study (1.39), but HHEP SF_{lin} (1.79) is slightly higher than SF_{lin} (1.12) in this study. This comparison suggests that HLM enzyme activities are similar between the two studies, but HHEP enzymes are slightly more active in this study than those in the publication (54).

For ECCS class 1A/1B, active uptake is typically involved through transporter-mediated mechanisms (OTAPs and OATs, Supplemental Material, Fig. S1). Traditionally, prediction of clearance for class 1A/1B compounds is to use transporter uptake assays to scale hepatic clearance, which can be quite challenging and variable (55–61). Our study indicates that clearance of class 1A/1B compounds can be scaled directly using metabolic clearance from suspension HEPs with higher SFs than class 2/4. The higher SFs may be accounting for the active uptake components by the transporters, although the detailed mechanisms involved are not entirely clear at this point. In practice, this approach simplifies the clearance prediction

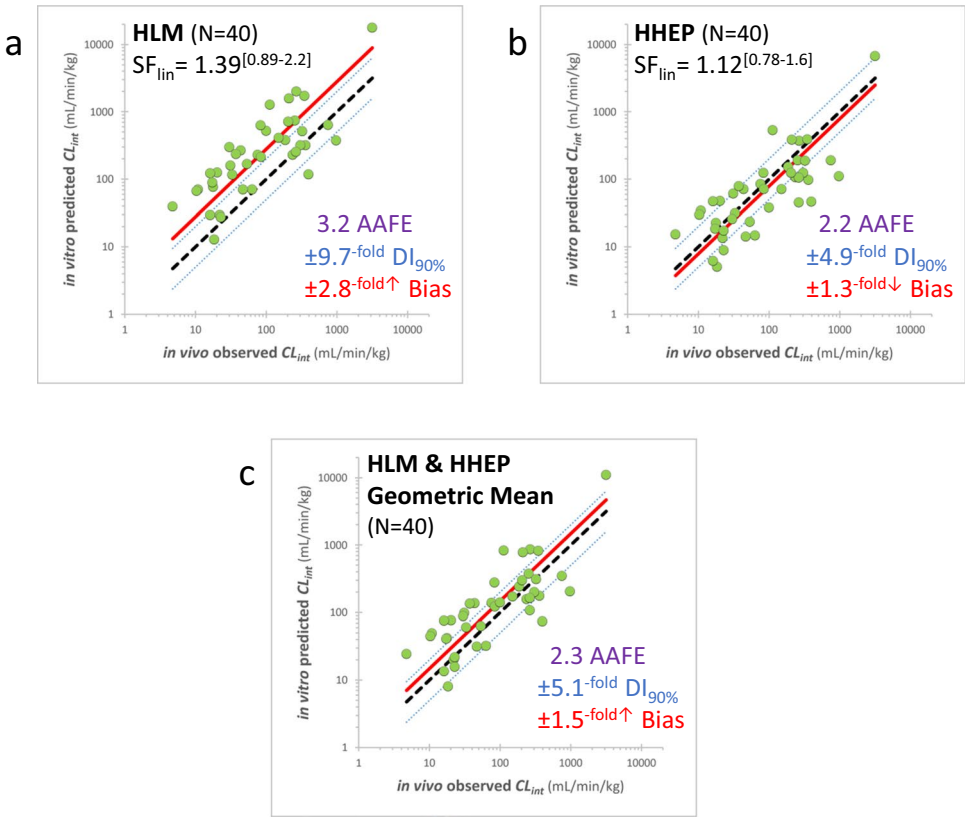

Fig. 6 Human liver microsome and hepatocyte intrinsic clearance disconnect (CL_{int} HLM/HHEP ≥ 2). **a** Using HLM CL_{int}, **b** Using HHEP CL_{int}, **c** Using geometric mean of HLM and HHEP CL_{int}

Table III Summary of Statistical Metrics of Intrinsic Clearance IVIVE Using HLM and HHEP based on ECCS Class for Compounds with HLM $CL_{int} > 2 \times$ HHEP CL_{int}

Species	Reagent	ECCS	*N*	SF_{lin}[a]	SF_{β}[a]	Bias[b,c] (AFE)	AAFE[b]	$DI_{90\%}$[b]	$P_{\leq 2\text{-fold}}$[b]	within 2-fold	ρ^{2b} (R^2)
Human	LM	2/4	40	1.39[fixed]	0[fixed]	2.8↑[2.2–3.6]	3.2[2.7–3.9]	9.7[7.0–14]	38%[33–44%]	30%	0.61[0.43–0.75]
	HEP	2/4	40	1.12[fixed]	0[fixed]	1.3↓[1.0–1.6]	2.2[1.9–2.6]	4.9[3.7–6.8]	53%[45–62%]	44%	0.60[0.41–0.74]
	LM&HEP Geomean	2/4	40			1.5↑[1.2–1.9]	2.3[2.0–2.6]	5.1[3.8–7.0]	52%[44–60%]	44%	0.62[0.44–0.76]

[a] *Scaling factor best fits[95% confidence intervals]*

[b] *Summary statistics[90% confidence intervals]*

[c] *Overprediction bias↑, underprediction bias↓*

for class 1A/1B, i.e., measurement of active uptake rate by transporters is no longer needed. Further investigation of the mechanistic implications of this observation will help better refine our approaches in the future for clearance prediction. The introduction of the SF_{β} is an empirical approach in order to improve the accuracy of clearance prediction for ECCS class 1A/1B compounds. The SF_{β} is intended to account for potentially albumin-facilitated update by transporters (20). However, the underlying mechanisms of incorporating the SF_{β} are not entirely clear at this point. Albumin-facilitated update is a topic that requires further research in the future. With the SF_{β}, the lower the $f_{u,p}$, the larger the clearance scaling factor. Drug discovery team may attempt to reduce plasma protein binding in order to lower clearance. However, clearance is not very sensitive to $f_{u,p}$ change. With SF_{β} for class 1A/1B compounds, 10-fold higher $f_{u,p}$ results in 3-fold decrease in intrinsic clearance. The unified set of SFs for both class 1A and 1B eliminate the need to identify the individual ECCS classification for each class prior to the clearance prediction. Identifying the transporters involved in the clearance of class 1A and 1B can be challenging for a number of reasons. High passive permeability can counter act the active uptake leading to minimal uptake signal *in vitro*, resulting in the active uptake not being detectable using HEK-293 cells transfected with uptake transporters (e.g., OATPs and OATs) or plated HHEP. To further elucidate OATP transporter involvement, *in vivo* non-human primate (NHP) drug-drug interaction (DDI) studies are often performed using single-dose rifampin administration (62). Occasionally, both OAT and OATP transporters are involved in the hepatic uptake of compounds making it challenging to decide the appropriate SFs to use to scale clearance for dual substrates of OAT and OATP. The current approach with the unified SFs for both class 1A and 1B simplifies the clearance prediction process and reduces the data required to select the appropriate SF. When making predictions for victim transporter DDIs at later stages of drug discovery, transporter reaction phenotyping becomes important.

Permeability-limited metabolism in HEP has recently been reported for ECCS class 2 compounds that are mainly metabolized by CYPs (17). This happens when metabolic rate is faster than permeation rate across the HEP membrane. In rats, for the CL_{int} LM > HEP compounds (permeability-limited), rat LM predicted *in vivo* clearance well (not permeability-limited) (38). The reason for the *in vitro-in vivo* differences are not fully understood but may suggest permeability-limited metabolism in rat HEP is an *in vitro* artifact. Rat HEP membrane permeation is no longer limiting metabolism *in vivo* as it can be *in vitro*. In humans, however, permeability limits metabolism to some extent *in vivo*, but not as severe as *in vitro*. For the dataset evaluated, HLM significantly overpredicted *in vivo* human clearance, while HHEP slightly underpredicted and HLM-HHEP CL_{int} geomean slightly overpredicted clearance in humans. For compounds with HLM-HHEP disconnect (CL_{int} HLM/HHEP ≥ 2-fold) that are mostly metabolized by CYPs and/or FMO, project specific strategies can be considered based on additional mechanistic understanding of the cause for the disconnect. Future studies evaluating disconnects between LM and HEP are required to help build in-depth understanding of the intricate role of permeability in limiting metabolism both *in vitro* and *in vivo* across different species.

In conclusion, clearance IVIVE and SFs have been successfully developed for human and preclinical species using LM and HEP. In general, the SF_{lin} for ECCS class 2/4 is small (~ 1–2) with the exceptions of rodents (~ 2–4), suggesting enzyme activities of our *in vitro* reagents are comparable with *in vivo* under physiological conditions. SF_{β} was introduced to improve clearance prediction accuracy and reduce biases for ECCS class 1A/1B compounds. For ECCS 2/4 compounds predominantly metabolized by CYPs/FMO with HLM clearance greater than HHEP, HLM significantly overpredicted *in vivo* clearance. Project specific strategies may be used to scale human clearance.

Supplementary Information The online version contains supplementary material available at https://doi.org/10.1208/s12248-023-00800-x.

Acknowledgements Authors greatly appreciate the input and discussion from Stefanus Steyn, Manthena Varma, and many Pfizer colleagues.

Author Contribution David Tess, George C. Chang, Christopher Keefer, Anthony Carlo, Rhys Jones, and Li Di all contributed to the following areas: substantial contributions to the conception or design of the work; or the acquisition, analysis, or interpretation of data for the work; and drafting the work or revising it critically for important intellectual content; and final approval of the version to be published; and agreement to be accountable for all aspects of the work in ensuring that questions related to the accuracy or integrity of any part of the work are appropriately investigated and resolved.

Data Availability All data generated or analysed during this study are included in this published article.

Declarations

Conflict of Interest The authors declare no competing interests.

References

1. Smith DA, Beaumont K, Maurer TS, Di L. Clearance in drug design. J Med Chem. 2019;62(5):2245–55. https://doi.org/10.1021/acs.jmedchem.8b01263.
2. Smith DA, Beaumont K, Maurer TS, Di L. Relevance of half-life in drug design. J Med Chem. 2018;61(10):4273–82. https://doi.org/10.1021/acs.jmedchem.7b00969.
3. Smith DA, Beaumont K, Maurer TS, Di L. Volume of distribution in drug design. J Med Chem. 2015;58(15):5691–8. https://doi.org/10.1021/acs.jmedchem.5b00201.
4. Benet LZ, Zia-Amirhosseini P. Basic principles of pharmacokinetics. Toxicol Pathol. 1995;23(2):115. https://doi.org/10.1177/019262339502300203.
5. van de Waterbeemd H, Smith DA, Beaumont K, Walker DK. Property-based design: optimization of drug absorption and pharmacokinetics. J Med Chem. 2001;44(9):1313–33. https://doi.org/10.1021/jm000407e.
6. Caldwell GW, Masucci JA, Yan Z, Hageman W. Allometric scaling of pharmacokinetic parameters in drug discovery: can human CL, Vss and t1/2 be predicted from in-vivo rat data? Eur J Drug Metab Pharmacokinet. 2004;29(2):133–43. https://doi.org/10.1007/bf03190588.
7. Huang Q, Riviere JE. The application of allometric scaling principles to predict pharmacokinetic parameters across species. Expert Opin Drug Metab Toxicol. 2014;10(9):1241–53. https://doi.org/10.1517/17425255.2014.934671.
8. Lin JH. Applications and limitations of interspecies scaling and in vitro extrapolation in pharmacokinetics. Drug Metab Dispos. 1998;26(12):1202–12.
9. Riede J, Poller B, Umehara K-i, Huwyler J, Camenisch G. New IVIVE method for the prediction of total human clearance and relative elimination pathway contributions from in vitro hepatocyte and microsome data. Eur J Pharm Sci. 2016;86:96–102. https://doi.org/10.1016/j.ejps.2016.02.022.
10. Obach RS. Prediction of human clearance of twenty-nine drugs from hepatic microsomal intrinsic clearance data: an examination of in vitro half-life approach and nonspecific binding to microsomes. Drug Metab Dispos. 1999;27(11):1350–9.
11. Hallifax D, Foster JA, Houston JB. Prediction of human metabolic clearance from in vitro systems: retrospective analysis and prospective view. Pharm Res. 2010;27(10):2150–61. https://doi.org/10.1007/s11095-010-0218-3.
12. Hosea NA, Collard WT, Cole S, Maurer TS, Fang RX, Jones H, et al. Prediction of human pharmacokinetics from preclinical information: comparative accuracy of quantitative prediction approaches. J Clin Pharmacol. 2009;49(5):513–33.
13. Chen Y, Jin JY, Mukadam S, Malhi V, Kenny JR. Application of IVIVE and PBPK modeling in prospective prediction of clinical pharmacokinetics: strategy and approach during the drug discovery phase with four case studies PROSPECTIVE Simcyp SIMULATION OF CLINICAL PK DATAY. CHEN ET AL. Biopharm Drug Dispos. 2012;33(2):85-98. https://doi.org/10.1002/bdd.1769.
14. Jones HM, Gardner IB, Watson KJ. Modelling and PBPK simulation in drug discovery. AAPS J. 2009;11(1):155–66. https://doi.org/10.1208/s12248-009-9088-1.
15. Davies M, Jones RDO, Grime K, Jansson-Lofmark R, Fretland AJ, Winiwarter S, et al. Improving the accuracy of predicted human pharmacokinetics: lessons learned from the AstraZeneca drug pipeline over two decades. Trends Pharmacol Sci. 2020;41(6):390–408. https://doi.org/10.1016/j.tips.2020.03.004.
16. Di L. The role of drug metabolizing enzymes in clearance. Expert Opin Drug Metab Toxicol. 2014;10(3):379–93. https://doi.org/10.1517/17425255.2014.876006.
17. Keefer C, Chang G, Carlo A, Novak JJ, Banker M, Carey J, et al. Mechanistic insights on clearance and inhibition discordance between liver microsomes and hepatocytes when clearance in liver microsomes is higher than in hepatocytes. Eur J Pharm Sci. 2020;155:105541. https://doi.org/10.1016/j.ejps.2020.105541.
18. Di L, Keefer C, Scott DO, Strelevitz TJ, Chang G, Bi Y-A, et al. Mechanistic insights from comparing intrinsic clearance values between human liver microsomes and hepatocytes to guide drug design. Eur J Med Chem. 2012;57:441–8. https://doi.org/10.1016/j.ejmech.2012.06.043.
19. Di L, Trapa P, Obach RS, Atkinson K, Bi Y-A, Wolford AC, et al. A novel relay method for determining low-clearance values. Drug Metab Dispos. 2012;40(9):1860–5. https://doi.org/10.1124/dmd.112.046425.
20. Jones RS, Leung C, Chang JH, Brown S, Liu N, Yan Z, et al. Application of empirical scalars to enable early prediction of human hepatic clearance using in vitro-in vivo extrapolation in drug discovery: an evaluation of 173 drugs. Drug Metab Dispos. 2022;50(8):1053–63. https://doi.org/10.1124/dmd.121.000784.
21. Chan TS, Yu H, Moore A, Khetani SR, Tweedie D. Meeting the challenge of predicting hepatic clearance of compounds slowly metabolized by cytochrome P450 using a novel hepatocyte model. HepatoPac Drug Metab Dispos. 2013;41(12):2024–32. https://doi.org/10.1124/dmd.113.053397.
22. Francis LJ, Houston JB, Hallifax D. Impact of plasma protein binding in drug clearance prediction: a database analysis of published studies and implications for in vitro-in vivo extrapolation. Drug Metab Dispos. 2021;49(3):188–201. https://doi.org/10.1124/dmd.120.000294.
23. Poulin P, Hop CECA, Ho Q, Halladay JS, Haddad S, Kenny JR. Comparative assessment of in vitro-in vivo extrapolation methods used for predicting hepatic metabolic clearance of drugs. J Pharm Sci. 2012;101(11):4308–26. https://doi.org/10.1002/jps.23288.
24. Poulin P, Haddad S. Toward a new paradigm for the efficient in vitro-in vivo extrapolation of metabolic clearance in humans from hepatocyte data. J Pharm Sci. 2013;102(9):3239–51. https://doi.org/10.1002/jps.23502.
25. Saravanakumar A, Sadighi A, Ryu R, Akhlaghi F. Physicochemical properties, biotransformation, and transport pathways of

established and newly approved medications: a systematic review of the top 200 most prescribed drugs *vs.* the FDA-approved drugs between 2005 and 2016. Clin Pharmacokinet. 2019;58(10):1281–94. https://doi.org/10.1007/s40262-019-00750-8.
26. Martignoni M, Groothuis GMM, de Kanter R. Species differences between mouse, rat, dog, monkey and human CYP-mediated drug metabolism, inhibition and induction. Expert Opin Drug Metab Toxicol. 2006;2(6):875–94. https://doi.org/10.1517/17425255.2.6.875.
27. Di L, Feng B, Goosen TC, Lai Y, Steyn SJ, Varma MV, et al. A perspective on the prediction of drug pharmacokinetics and disposition in drug research and development. Drug Metab Dispos. 2013;41(12):1975–93. https://doi.org/10.1124/dmd.113.054031.
28. Mathew S, Tess D, Burchett W, Chang G, Woody N, Keefer C, et al. Evaluation of prediction accuracy for volume of distribution in rat and human using in vitro, in vivo, PBPK and QSAR methods. J Pharm Sci (Philadelphia, PA, U S). 2021;110(4):1799–823. https://doi.org/10.1016/j.xphs.2020.12.005.
29. Di L, Artursson P, Lennernas H, Avdeef A, Benet L, Houston B, et al. The critical role of passive permeability in designing successful drugs. ChemMedChem. 2020;15(20):1862–74. https://doi.org/10.1002/cmdc.202000419.
30. Di L, Rong H, Feng B. Demystifying brain penetration in central nervous system drug discovery. J Med Chem. 2013;56(1):2–12. https://doi.org/10.1021/jm301297f.
31. Nigade PB, Gundu J, Pai KS, Nemmani KVS, Talwar R. Prediction of volume of distribution in preclinical species and humans: application of simplified physiologically based algorithms. Xenobiotica. 2019;49(5):528–39. https://doi.org/10.1080/00498254.2018.1474399.
32. Jones RD, Jones HM, Rowland M, Gibson CR, Yates JWT, Chien JY, et al. PhRMA CPCDC initiative on predictive models of human pharmacokinetics, Part 2: Comparative assessment of prediction methods of human volume of distribution. J Pharm Sci. 2011;100(10):4074–89. https://doi.org/10.1002/jps.22553.
33. Price E, Kalvass JC, DeGoey D, Hosmane B, Doktor S, Desino K. Global analysis of models for predicting human absorption: QSAR, in vitro, and preclinical models. J Med Chem. 2021;64(13):9389–403. https://doi.org/10.1021/acs.jmedchem.1c00669.
34. Paine SW, Menochet K, Denton R, McGinnity DF, Riley RJ. Prediction of human renal clearance from preclinical species for a diverse set of drugs that exhibit both active secretion and net reabsorption. Drug Metab Dispos. 2011;39(6):1008–13. https://doi.org/10.1124/dmd.110.037267.
35. Mahmood I. Interspecies scaling of renally secreted drugs. Life Sci. 1998;63(26):2365–71. https://doi.org/10.1016/s0024-3205(98)00525-6.
36. Jansen K, Pou Casellas C, Groenink L, Wever KE, Masereeuw R. Humans are animals, but are animals human enough A systematic review and meta-analysis on interspecies differences in renal drug clearance. Drug Discovery Today. 2020;25(4):706–17. https://doi.org/10.1016/j.drudis.2020.01.018.
37. Riley RJ, McGinnity DF, Austin RP. A unified model for predicting human hepatic, metabolic clearance from in vitro intrinsic clearance data in hepatocytes and microsomes. Drug Metab Dispos. 2005;33(9):1304–11.
38. Tess DA, Ryu S, Di L. In vitro - in vivo extrapolation of hepatic clearance in preclinical species. Pharm Res. 2022;39(7):1615–32. https://doi.org/10.1007/s11095-022-03205-1.
39. Varma MV, Steyn SJ, Allerton C, El-Kattan AF. Predicting clearance mechanism in drug discovery: extended clearance classification system (ECCS). Pharm Res. 2015;32(12):3785–802. https://doi.org/10.1007/s11095-015-1749-4.
40. Lombardo F, Berellini G, Scott OR. Trend analysis of a database of intravenous pharmacokinetic parameters in humans for 1352 drug compounds. Drug Metab Dispos. 2018;46(11):1466–77. https://doi.org/10.1124/dmd.118.082966.
41. Li AP, Lu C, Brent JA, Pham C, Fackett A, Ruegg CE, et al. Cryopreserved human hepatocytes: characterization of drug-metabolizing enzyme activities and applications in higher throughput screening assays for hepatotoxicity, metabolic stability, and drug-drug interaction potential. Chem Biol Interact. 1999;121(1):17–35. https://doi.org/10.1016/s0009-2797(99)00088-5.
42. Beal SL. Ways to fit a PK model with some data below the quantification limit. J Pharmacokinet Pharmacodyn. 2001;28(5):481–504.
43. Di L, Whitney-Pickett C, Umland JP, Zhang H, Zhang X, Gebhard DF, et al. Development of a new permeability assay using low-efflux MDCKII cells. J Pharm Sci. 2011;100(11):4974–85.
44. Novak JJ, Di L, Burchett W. Effects of low temperature on blood-to-plasma ratio measurement. Biopharm Drug Dispos. 2021;42(5):234–41.
45. Chang G, Woody N, Keefer C. Providing the 'best' lipophilicity assessment in a drug discovery environment. ChemRxiv. 2021. https://doi.org/10.26434/chemrxiv.14292485.v1.
46. Hay T, Jones R, Beaumont K, Kemp M. Modulation of the partition coefficient between octanol and buffer at pH 7.4 and pKa to achieve the optimum balance of blood clearance and volume of distribution for a series of tetrahydropyran histamine type 3 receptor antagonists. Drug Metab Dispos. 2009;37(9):1864–70. https://doi.org/10.1124/dmd.109.027888.
47. Lombardo F, Shalaeva MY, Tupper KA, Gao F. ElogDoct: a tool for lipophilicity determination in drug discovery. 2. Basic and Neutral Compounds. J Med Chem. 2001;44(15):2490–7. https://doi.org/10.1021/jm0100990.
48. Li R, Bi Y-A, Lai Y, Sugano K, Steyn SJ, Trapa PE, et al. Permeability comparison between hepatocyte and low efflux MDCKII cell monolayer. AAPS J. 2014;16(4):802–9. https://doi.org/10.1208/s12248-014-9616-5.
49. Shalaeva M, Kenseth J, Lombardo F, Bastin A. Measurement of dissociation constants (pKa values) of organic compounds by multiplexed capillary electrophoresis using aqueous and cosolvent buffers. J Pharm Sci. 2008;97(7):2581–606. https://doi.org/10.1002/jps.21287.
50. Poole SK, Patel S, Dehring K, Workman H, Poole CF. Determination of acid dissociation constants by capillary electrophoresis. J Chromatogr A. 2004;1037(1–2):445–54. https://doi.org/10.1016/j.chroma.2004.02.087.
51. Lin LI-K. Measuring Agreement. In: Chow S-c, editor. Encyclopedia of Biopharmaceutical Statistics 3rd ed. London, UK: Informa UK Limited; 2010. p. 745–50.
52. Agarwal P, Ishida K, Reid DL, Gupta A. Clearance prediction for Amgen molecules against Extended Clearance Classification System (ECCS) and future directions. Drug Discov Today. 2021;26(1):10–6. https://doi.org/10.1016/j.drudis.2020.10.008.
53. Wood FL, Houston JB, Hallifax D. Clearance prediction methodology needs fundamental improvement: trends common to rat and human hepatocytes/microsomes and implications for experimental methodology. Drug Metab Dispos. 2017;45(11):1178–88.
54. Williamson B, Harlfinger S, McGinnity DF. Evaluation of the disconnect between hepatocyte and microsome intrinsic clearance and in vitro in vivo extrapolation performance. Drug Metab Dispos. 2020;48(11):1137–46. https://doi.org/10.1124/dmd.120.000131.
55. Jones HM, Barton HA, Lai Y, Bi Y-a, Kimoto E, Kempshall S, et al. Mechanistic pharmacokinetic modeling for the prediction of transporter-mediated disposition in humans from sandwich culture human hepatocyte data. Drug Metab Dispos. 2012;40(5):1007–17. https://doi.org/10.1124/dmd.111.042994.
56. Li R, Barton HA, Yates PD, Ghosh A, Wolford AC, Riccardi KA, et al. A "middle-out" approach to human pharmacokinetic

predictions for OATP substrates using physiologically-based pharmacokinetic modeling. J Pharmacokinet Pharmacodyn. 2014;41(3):197–209. https://doi.org/10.1007/s10928-014-9357-1.
57. Ménochet K, Kenworthy KE, Houston JB, Galetin A. Use of mechanistic modeling to assess interindividual variability and interspecies differences in active uptake in human and rat hepatocytes. Drug Metab Dispos. 2012;40(9):1744–56. https://doi.org/10.1124/dmd.112.046193.
58. Kumar V, Yin M, Ishida K, Salphati L, Hop C, Rowbottom C, et al. Prediction of transporter-mediated rosuvastatin hepatic uptake clearance and drug interaction in humans using proteomics-informed REF approach. Drug Metab Dispos. 2021;49(2):159–68. https://doi.org/10.1124/dmd.120.000204.
59. Lee W, Koyama S, Morita K, Kiriake A, Kikuchi R, Chu X, et al. Cell-to-medium concentration ratio overshoot in the uptake of statins by human hepatocytes in suspension, but not in monolayer: kinetic analysis suggesting a partial loss of functional OATP1Bs. AAPS J. 2020;22(6):133. https://doi.org/10.1208/s12248-020-00512-6.
60. Yoshikado T, Lee W, Toshimoto K, Morita K, Kiriake A, Chu X, et al. Evaluation of hepatic uptake of OATP1B substrates by short term-cultured plated human hepatocytes: comparison with isolated suspended hepatocytes. J Pharm Sci. 2021;110(1):376–87. https://doi.org/10.1016/j.xphs.2020.10.041.
61. Mao J, Doshi U, Wright M, Hop C, Li AP, Chen Y. Prediction of the pharmacokinetics of pravastatin as an OATP substrate using plateable human hepatocytes with human plasma data and PBPK modeling. CPT Pharmacometrics Syst Pharmacol. 2018;7(4):251–8. https://doi.org/10.1002/psp4.12283.
62. Tess DA, Eng H, Kalgutkar AS, Litchfield J, Edmonds DJ, Griffith DA, et al. Predicting the human hepatic clearance of acidic and zwitterionic drugs. J Med Chem. 2020;63(20):11831–44. https://doi.org/10.1021/acs.jmedchem.0c01033.